Kerr-Lens Mode-Locked 2-μm Thin-Disk Lasers

Jinwei Zhang, Ka Fai Mak, and Oleg Pronin

(Invited Paper)

***Abstract*—Thin-disk technology uniquely enables the simultaneous scaling of both average and peak powers, while maintaining an excellent beam profile. It has been widely adopted in the 1-μm region, not only for continuous wave lasers but also for pulsed oscillators and amplifiers. However, the development of 2-μm thin-disk lasers is still at a very early stage, with passive mode locking having been demonstrated only recently. Here, we describe in detail a new femtosecond Ho:YAG thin-disk oscillator and recent power-scaling experiments that resulted in an average power of up to 25 W—the highest average power of any mode-locked oscillator in the 2-μm region. The future directions toward even higher average and peak power thin-disk oscillators are also discussed.**

***Index Terms*—Kerr-lens mode locking (KLM), ultrafast lasers, thin-disk lasers, Ho:YAG, mid-infrared lasers.**

I. Introduction

ULTRAFAST lasers at 2 μm have enabled diverse applications ranging from material processing, remote sensing to medical use [1]–[4], and can facilitate the effective generation of coherent radiation in other spectral regions that are not easily accessible. For example, soft X-rays can be generated via high harmonic generation (HHG), with the obtained X-ray photon energy proportional to $\sim\lambda^2$, where λ is the wavelength of the HHG driving pulse [5]–[7]. Obviously, replacing the commonly used near-infrared pump with a mid-infrared driver will deliver higher photon energies, albeit at a reduced conversion efficiency. The spectrally coherent nature of the generated radiation, whether X-ray or mid-infrared, mean not only frequency domain applications such as X-ray and XUV spectroscopy can tremendously benefit from such sources, but also time-domain applications such as frequency comb spectroscopy, attosecond pulse generation and pump-probe spectroscopy [8].

Coherent mid-infrared can be generated using 2 μm ultrafast lasers via parametric processes in nonlinear crystals [9]. The concept has been extensively studied using near-infrared sources [10]–[13] as they are already available in many research labs. Nevertheless, these studies show the significant limitations inherent in near-infrared pumping for mid-infrared generation. Highly nonlinear non-oxide crystals such as GaSe and AgGaSe, for example, transmit up to 25 μm and even to the low THz range [14]. Yet, due to their smaller bandgap, they can only withstand high power and generate meaningful throughput when pumped at wavelengths at 1.2 μm or longer to minimize two- or three-photon absorptions [15]. By pumping at 2 μm, much higher mid-infrared generation efficiencies can be expected [16]. Coincidentally, for GaSe, a pump wavelength around 2 μm also corresponds to a very broad phase-matching bandwidth that spans multiple octaves in the mid-infrared [17], [18]. The required powerful 2 μm pump light can in principle be generated from standard ultrafast 1 μm sources via cascaded down-conversion schemes [12], [19], but it tends to increase noise and compromise efficiency. To directly reach the long-wave infrared (5–20 μm) using mature 1 μm sources as a direct pump, wide-bandgap crystals with comparatively low nonlinearities [11] such as LGS can be employed. They provide, however, two orders of magnitude lower figure of merit [12] when compared to the direct pumping of GaSe at 2 μm, highlighting the enormous advantage of using high power 2 μm sources.

There are numerous laser gain media emitting around 2 μm such as Cr:ZnSe/ZnS, Tm/Ho doped bulk crystals and Tm/Ho doped fibers. Femtosecond fiber oscillators [20], [21] can only deliver limited power and usually require further amplification [22], [23]. Such oscillator-amplifier systems have delivered the highest average power achieved in the 2 μm region to date [22]. Oscillators based on Cr:ZnSe/ZnS bulk crystals can directly deliver 2 W of average power at few tens of femtosecond pulse durations [24]–[27], but the strong thermal effects in ZnSe/ZnS crystals hinder further power scaling. Another promising candidate for generating high power ultrashort pulses is Ho:YAG crystal due to its low quantum defect (absorption around 1.9 μm), good crystal quality and still relatively broad emission bandwidth. It has been utilized in q-switched and actively mode-locked systems [28], [29], and recently also in a passively mode-locked oscillator using semiconductor saturable absorber mirrors (SESAMs) [30], [31]. However, the output power and pulse duration were limited respectively to only several hundred milliwatts and few picoseconds.

Thin-disk technology is one of the common routes to generate high average power, high peak power and high energy pulses [32]. Since its invention it has been successfully utilized in the development of Yb-doped mode-locked oscillators, with peak and average powers scaled to unprecedented values approaching 60 MW and 300 W respectively [33]–[36]. Compared to 1 μm thin-disk lasers, the development of 2 μm thin-disk lasers is, nevertheless, still at an early stage, with only continuous wave (CW) operations demonstrated until recently [9] based

Manuscript received December 18, 2017; revised February 22, 2018; accepted March 6, 2018. Date of publication March 9, 2018; date of current version April 3, 2018. This work was supported in part by the Munich-Centre for Advanced Photonics and in part by the Center for Advanced Laser Applications. *(Corresponding author: Jinwei Zhang.)*

The authors are with the Max Planck Institute of Quantum Optics, 85748 Garching, Germany (e-mail: jinwei.zhang@mpq.mpg.de; kafai.mak@mpq.mpg.de; oleg.pronin@mpq.mpg.de).

Color versions of one or more of the figures in this paper are available online at http://ieeexplore.ieee.org.

Digital Object Identifier 10.1109/JSTQE.2018.2814780

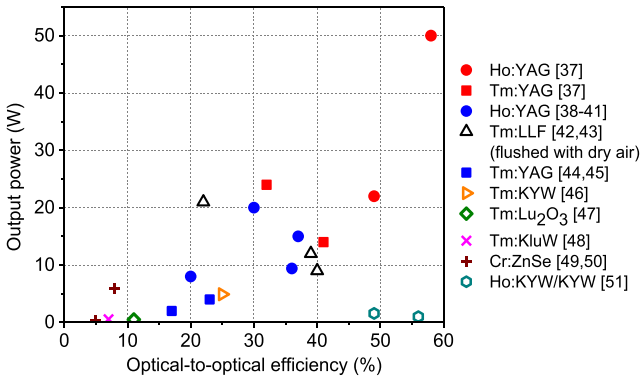

Fig. 1. Overview of the different CW multimode regimes of operation. The picture is adopted from [37].

on different combinations of Tm or Ho doped host crystals such as YAG, YLF, KYW, and LLF_4. Transition-metal doped II-VI semiconductor laser materials such as Cr:ZnSe have also been experimentally realized in thin-disk geometry, albeit with relatively limited output due to significant thermal issues. An overview of the published results on CW thin-disk lasers emitting around 2 μm is shown in Fig. 1 [37]. It can be seen that Ho:YAG thin-disk lasers can deliver much higher average powers at much greater efficiencies than other gain media under CW operation, demonstrating its great potential for further average power scaling [37]–[51].

In 1 μm thin-disk oscillators, both SESAM [52] and Kerr-lens mode locking (KLM) [33] are widely used to generate ultrashort pulses. Compared to SESAM, the use of KLM is advantages for generating shorter pulses due to its fast response time and relatively large modulation depth. This is confirmed in the case of Yb:YAG thin-disk oscillator, where KLM generated pulses four times shorter than those obtained via SESAM mode-locking. The absence of linear losses in KLM also facilitates high intracavity average power and is especially advantageous when both high intra-cavity peak and average powers are simultaneously generated. The key element in KLM is a transparent medium exhibiting sufficient nonlinearity for self-focusing at the laser wavelength. A sapphire crystal is usually sufficient, making this technique cost effective and highly accessible. Importantly, the KLM method is wavelength independent and, thus, can be applied to different spectral ranges with very little modifications. In this work, we combine thin-disk technology, the KLM technique and Ho:YAG gain medium to develop a new class of mode-locked oscillators around 2 μm wavelength.

II. KLM Ho:YAG Thin-Disk Oscillator With Four-Pass Configuration

In this paper, a four-pass configuration is defined as a configuration where the laser beam propagates through the thin-disk four times per cavity round-trip, as shown in Fig. 2.

A. Oscillator Setup

The schematic of the first mode-locked oscillator is shown in Fig. 2. The 200 μm thin Ho:YAG disk has a Ho^{3+} doping concentration of 2.5%, and is mounted on a water cooled heat sink placed inside a 72-pass pump head. The disk's front surface is antireflection coated for the pump and laser emission wavelengths, and the back side has a high reflective coating for both wavelengths ($R > 99.9\%$). The disk is slightly wedged to separate any residual reflections off the front surface from the main beam. A Tm-fiber laser capable of providing 120 W of output power at 1908 nm wavelength is used as the pump source. Rather than directly sent to the thin-disk module, the single-mode pump light is coupled through a 550 μm diameter multimode fiber—at an efficiency of 80%—to homogenize the pump spot and to prevent damaging the pump head's internal optics due to small foci. It also serves as a very effective isolator preventing the back reflected light from the disk module from re-entering the pump fiber laser. The resulting pump spot diameter on the disk is $\sim$3 mm. The ratio between the pump spot diameter to the disk thickness is larger than ten, allowing optimal thin-disk operation with advantages one dimensional heat flow [32].

The Ho:YAG thin disk is placed as a folding mirror within a Z-shape cavity. A 1-mm-thick sapphire plate is placed in the focus between the two concave mirrors (R1 and R2) to act as a Kerr medium, providing the necessary Kerr-lens effect for mode-locking. The total anomalous group delay dispersion (GDD) per round trip is $-16000\,fs^2$, introduced by a pair of chirped mirrors with four bounces on each surface. The dispersive mirrors were described in detail in [53]. Crucial for high-power applications, these mirrors had losses below 0.05% and did not exhibit any thermal effects under 0.9 kW of intra-cavity average power. A water cooled copper plate with a circular hole is placed near one of the end mirrors to act as a hard aperture and to aid the stabilization of Kerr-lens mode locking. The total cavity length is $\sim$1730 mm, corresponding to a repetition rate of 86.5 MHz. Generally, the cavity configuration is similar to the one implemented for Yb:YAG thin-disk oscillators [54]. Yet due to the comparatively low gain of Ho:YAG, the oscillator is rather sensitive to the overall cavity loss, resulting in different behaviors under different output coupling ratios. Fig. 3(a) shows the cavity mode when the oscillator is operated close to the stability edge where mode locking was realized. Fig. 3(b) shows the beam radius on the thin disk as a function of the separation distance between the two concave mirrors, indicating the range of the stability zone, in both the CW and ML regime.

B. Operation With 1% OC

The initial investigation on KLM was conducted using a low output coupling ratio of 1%, such that a high intracavity power and a correspondingly strong Kerr-lensing can be established. The oscillator was first operated in the CW regime, close to the center of the cavity stability zone (Fig. 3(b)). At 1% output coupling, an average output power of up to 9.2 W was reached at an estimated absorbed pump power of 80 W (see Fig. 4(a)). The corresponding intracavity average power was 920 W. The pump power was then decreased to 58 W for mode-locking experiments, where the output power was 7 W. In order to initiate KLM, one of the concave mirrors was shifted towards the

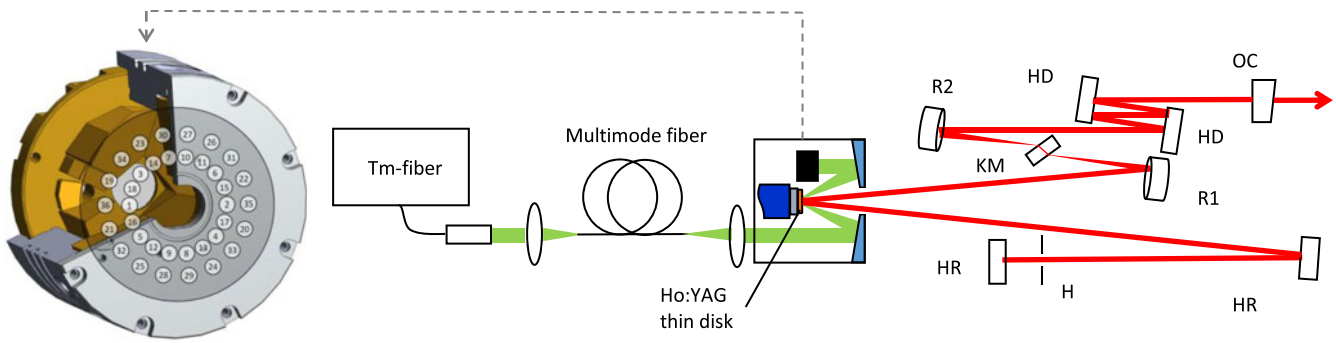

Fig. 2. Schematic of the oscillator setup of the four-pass configuration. HR: High-reflection mirror, R1 and R2: concave spherical mirrors with radius of curvature (ROC) of –100 mm, KM: Kerr medium, HD: highly dispersive chirped mirror, H: hard aperture, OC: Output coupler. Left: Schematic of the 72-pass pump cavity. The numbers represent the sequential pump beam locations on the parabolic mirror. Courtesy of TRUMPF Laser GmbH.

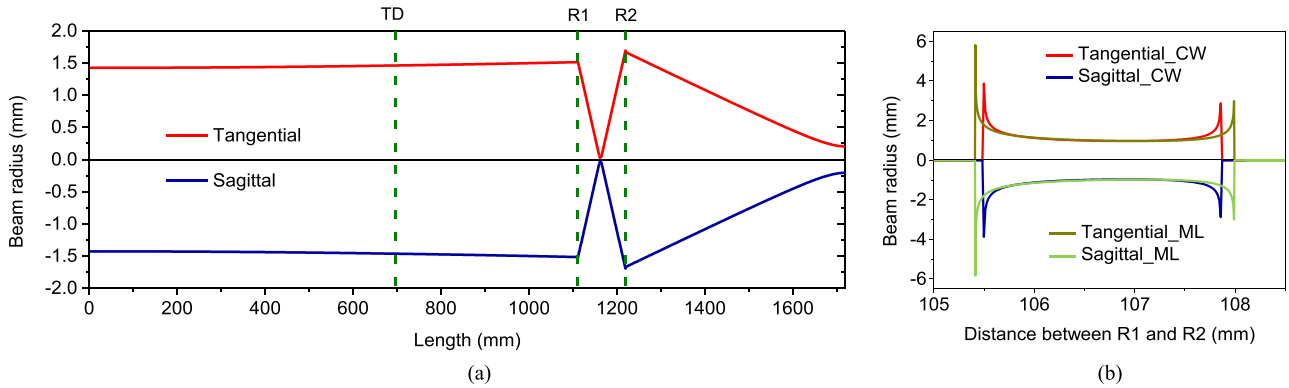

Fig. 3. (a) Cavity mode within the four-pass configuration when the distance between R1 and R2 equals to 105.7 mm. The dotted lines show the position of the thin disk and concave mirrors. (b) Dependence of the thin-disk beam radius on the separation distance between the concave mirrors (R1 and R2) in both CW and ML operations. Mode locking is realized close to the stability edge around 105.7 mm with an estimated Kerr-lens focal length of ∼30 mm.

stability edge to increase the sensitivity of the laser mode to the Kerr-lens effect, resulting in a drop of CW average power to 6.5 W. Mode-locking was triggered by perturbing the OC mounted on a translation stage. The perturbation of this end-mirror does not lead to any misalignments and can be repeatedly performed. The average output power decreased to 6.2 W after mode locking, corresponding to an intra-cavity average power of 620 W, and an optical-to-optical efficiency of 10.6%. The mode-locked spectrum (Fig. 4(b)) measured using a Fourier transform infrared (FTIR) spectrometer was centered at 2093 nm with a full width at half maximum (FWHM) bandwidth of 14 nm, covering a significant portion of the Ho:YAG crystal's emission spectrum (Fig. 4(b)). Fig. 4(c) shows the pulse trace measured with an intensity autocorrelator. The pulse duration, at 410 fs assuming a sech^2 shape fit, indicates a nearly Fourier-transform-limited pulse with a time-bandwidth product of 0.39.

The radio frequency (RF) spectrum was measured using a RF spectrum analyzer at a resolution bandwidth of 100 Hz. The fundamental beat note, located at 86.5 MHz as expected given the cavity length, has a signal-to-noise ratio of 73 dB (see Fig. 4(d)). Despite the limited optimization on the setup's mechanical stability, KLM operation can be maintained for several hours on a day-to-day basis under ambient air conditions and different levels of air humidity.

C. Operation With 1.8% OC

Having demonstrated mode-locked operation using the 1% output coupler, the usable output power was raised by increasing the output coupling to 1.8%. At the center of the stability zone, the intracavity laser power, at 1.06 kW, was similar to the previous case, but the output laser power was more than doubled, reaching 19 W at an estimated absorbed pump power of 87 W (see Fig. 4(a)). Moving to the cavity stability edge as described in the previous case and using a lower pump power of 83 W, mode-locking could again be achieved, delivering an average output power of 16 W, slightly lower than the CW output power before mode locking (16.4 W). However, this output contains not only the mode-locked spectrum, but also a CW component, located at the main emission peak of Ho:YAG at 2092 nm (Fig. 4(b)). Two Kelly sidebands can also be seen at 2060 nm and 2100 nm. The FWHM bandwidth of the mode-locked spectrum is 14 nm when the CW spike is ignored, and is nearly identical to the 1% OC case. The autocorrelation measurement indicates a pulse duration of 400 fs assuming a sech^2 pulse shape (Fig. 4(c)). The RF spectrum for the 1.8% OC case shows an increase in noise compared to the 1% OC case (Fig. 4(d)) due to the presence of the CW spike.

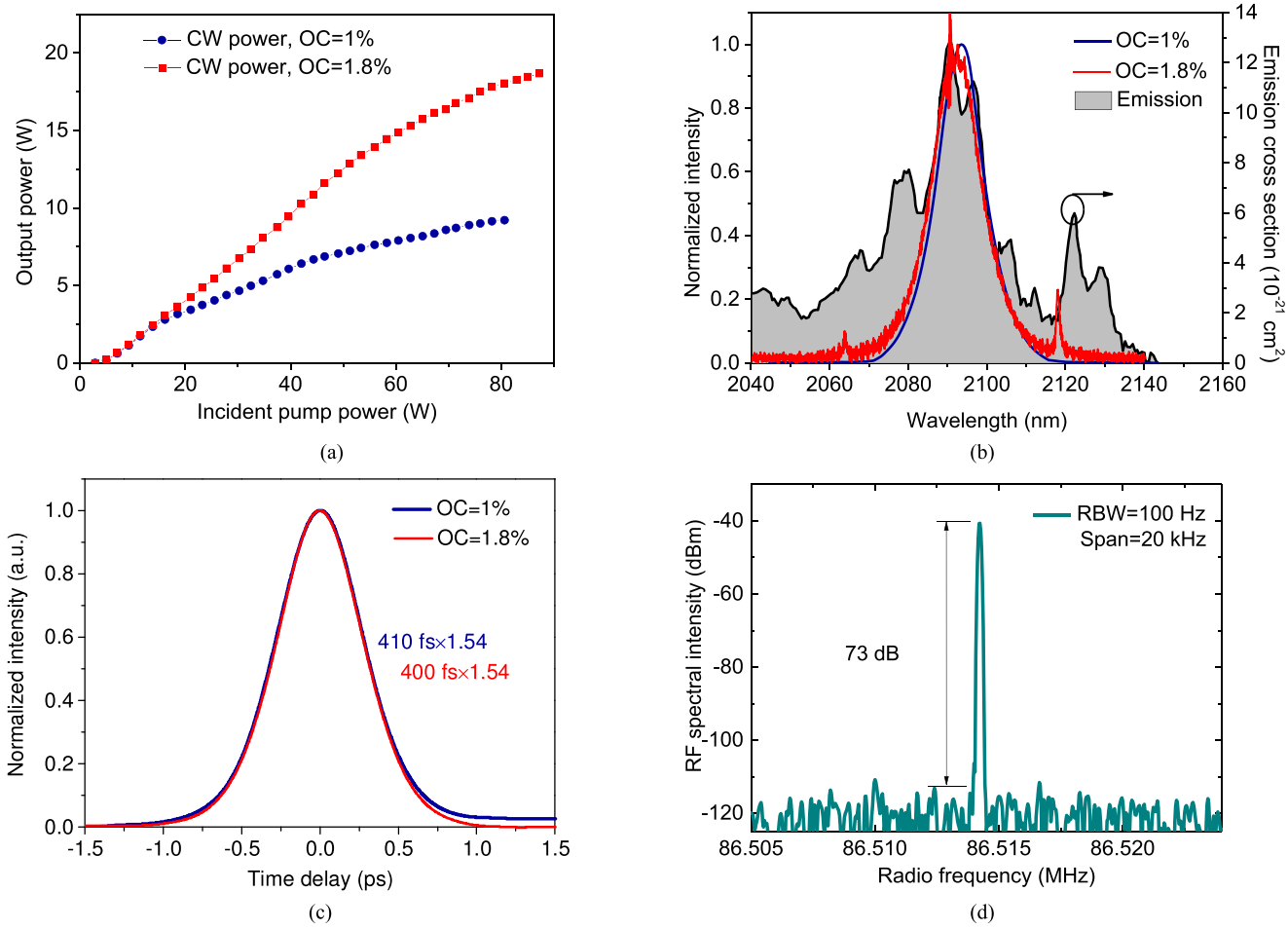

Fig. 4. Output parameters for the four-pass configuration. (a) CW output power versus incident pump power with the OC of 1% and 1.8%. (b) Mode-locked spectrum. (c) Intensity autocorrelation trace of pulses with the OC of 1% and 1.8%. (d) Radio frequency spectrum with RBW of 100 Hz for the 1% OC.

The appearance of the CW spike is a result of the increased intra-cavity power compared to the 1% OC case. However, when the power was lowered in an attempt to eliminate the spike, mode-locking could not be sustained due to the higher cavity loss, pointing to the need for higher gain in the cavity. A common way to increase the cavity gain for 1 μm thin-disk lasers is to increase the number of times the laser beam passes through the thin disk within one round trip [34]. In the next section the implementation of this method for the Ho:YAG thin-disk oscillator will be discussed.

III. KLM Ho:YAG Thin-Disk Oscillator With Eight-Pass Configuration

A. Oscillator Setup

The previous experiments verified the feasibility of KLM in a Ho:YAG thin-disk oscillator, and demonstrated intra-cavity average and peak powers of ~600 W and 15 MW respectively. These record intra-cavity average and peak powers showcase the huge potential of this technology to provide even higher output powers when higher gain and, thus, higher output coupling ratios can be implemented. An obvious step to this end is to increase the number of passes through the disk. Thus, the number of passes was doubled to eight. This eight-pass configuration was realized by using a pair of 45-degree mirrors (see Fig. 5), which folded the beam path through the thin Ho:YAG disk. This boosted the round-trip gain and enabled the use of higher output coupling ratios, which is also beneficial for increasing the optical-to-optical efficiency [34]. The total cavity length was increased to ~1960 mm, corresponding to a repetition rate of 77 MHz. Fig. 6 shows the cavity mode of the oscillator operated close to the stability edge, and the range of the stability zone and the beam size on the thin disk within the whole stability zone.

B. Operation With Different OCs

To investigate the difference between the four-pass and eight-pass configuration, output couplers with 1% and 1.8% transmission were used again for both CW and mode-locked operation. An additional OC of 3% was also tried in an attempt to obtain higher average powers. Fig. 7(a) shows the CW operation of the oscillator with the three different output couplers. The maximum output powers in the stability center were 7.2 W, 14 W and 20 W at the respective output coupling ratios of 1%, 1.8% and 3%. Compared to the four-pass configuration, the CW powers did not

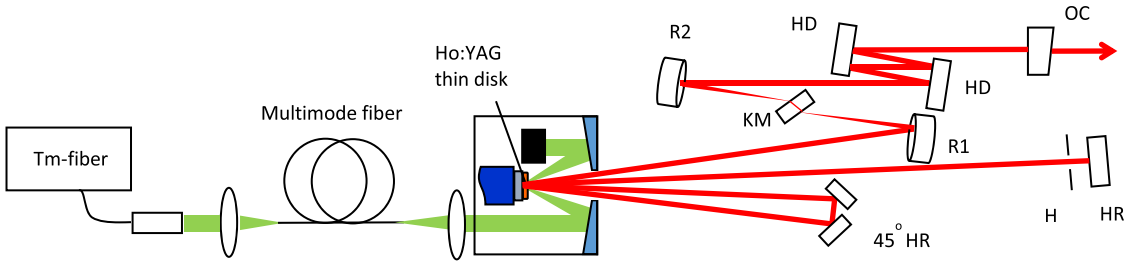

Fig. 5. Schematic of the oscillator setup with the eight-pass configuration.

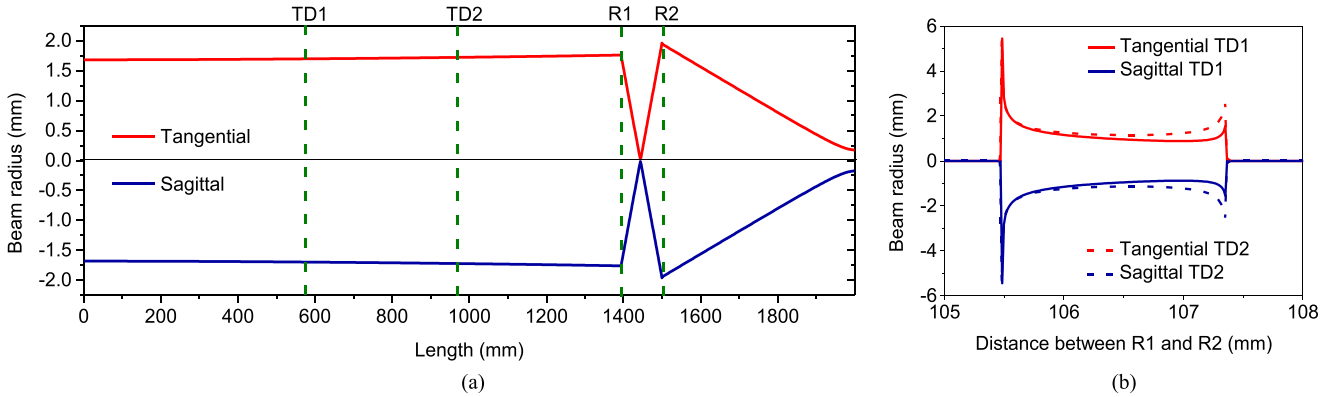

Fig. 6. (a) Cavity mode within the eight-pass configuration when the distance between R1 and R2 equals to 105.6 mm. TD1 and TD2 represent the two positions where the laser beam reflects from the thin disk. (b) Dependence of the beam radius at the two different disk positions on the separation distance between the concave mirrors (R1 and R2). Mode locking is realized close to the stability edge around 105.6 mm.

increase as one would expect, but was reduced for a given OC ratio. This is likely because the laser beam now goes through the thin disk two times more than in the four-pass configuration, making the cavity mode more sensitive to the detrimental thermal effects of the thin disk. This influence becomes more obvious at increased pump powers (Fig. 7(a)). However, it is also difficult to completely exclude the thermal effects originating from the dispersive mirrors and Kerr-medium.

Following the same procedure introduced in Section II and moving closer to the stability edge for initiating mode-locking, output powers of 5 W, 11 W and 17 W were obtained. Kerr-lens mode locking can be realized with all three output couplings, and the mode-locked output powers were 5.8 W (1%), 12 W (1.8%) and 18.4 W (3%), corresponding to optical-to-optical efficiencies of 10.4%, 16.7% and 22.2%, respectively. It is worth noting that, due to mirror leakage, a total of approximately 1.6 W was also measured behind the two 45-degree mirrors in all three cases, which can be reduced in the future by using mirrors with higher reflectivities.

The mode-locked spectra and intensity autocorrelation traces are shown in Fig. 7(b) and (c). The spectra corresponding to the three different output coupling ratios are nearly the same with FWHM bandwidths of $\sim$22 nm. In contrast to the four-pass configuration, no CW-spike was observed at the main emission peak at 2092 nm in any of the spectra. Nevertheless all the spectra contained a small CW peak at 2150 nm, which are presumably Kelly sidebands. The lack of a corresponding CW peak at shorter wavelengths is possibly due to the different higher order phases and reabsorption at shorter wavelengths. The pulse durations were measured to be 220 fs (1%), 230 fs (1.8%) and 220 fs (3%), indicating nearly Fourier-transform-limited pulses. These durations are almost halved compared to those in the four-pass oscillator. The RF spectrum, measured for the cavity with a 3% OC, is shown in the inset figure of Fig. 7(c) and indicates stable mode locking. The output beam has an excellent beam profile, and the measured M^2 factor is 1.05 for both the X and Y directions (Fig. 7(d)).

Compared to the four-pass oscillator, the higher gain provided by the eight passes did not result in higher output powers in the CW regime due to the increased sensitivity to thermal lensing. However, and importantly, it supports the realization of KLM at higher output coupling ratios. Besides, the modulation depth is larger for the eight-pass configuration due to the enhanced soft aperture effect as the laser beam interacts with the pump spot more frequently. As a result, the mode-locked spectra are much broader than those in the four-pass case, and is even broader, in terms of FWHM, than the emission peak of the Ho:YAG crystal, resulting in the shortening of pulse durations.

C. Operation With 4% OCs Transmission and Higher Pump Power

To further increase the average output power, higher output couplings and pump powers are needed. However, a single pump source can only provide a maximum power of 120 W, of which 96 W could be transmitted onto the disk. Fortunately the

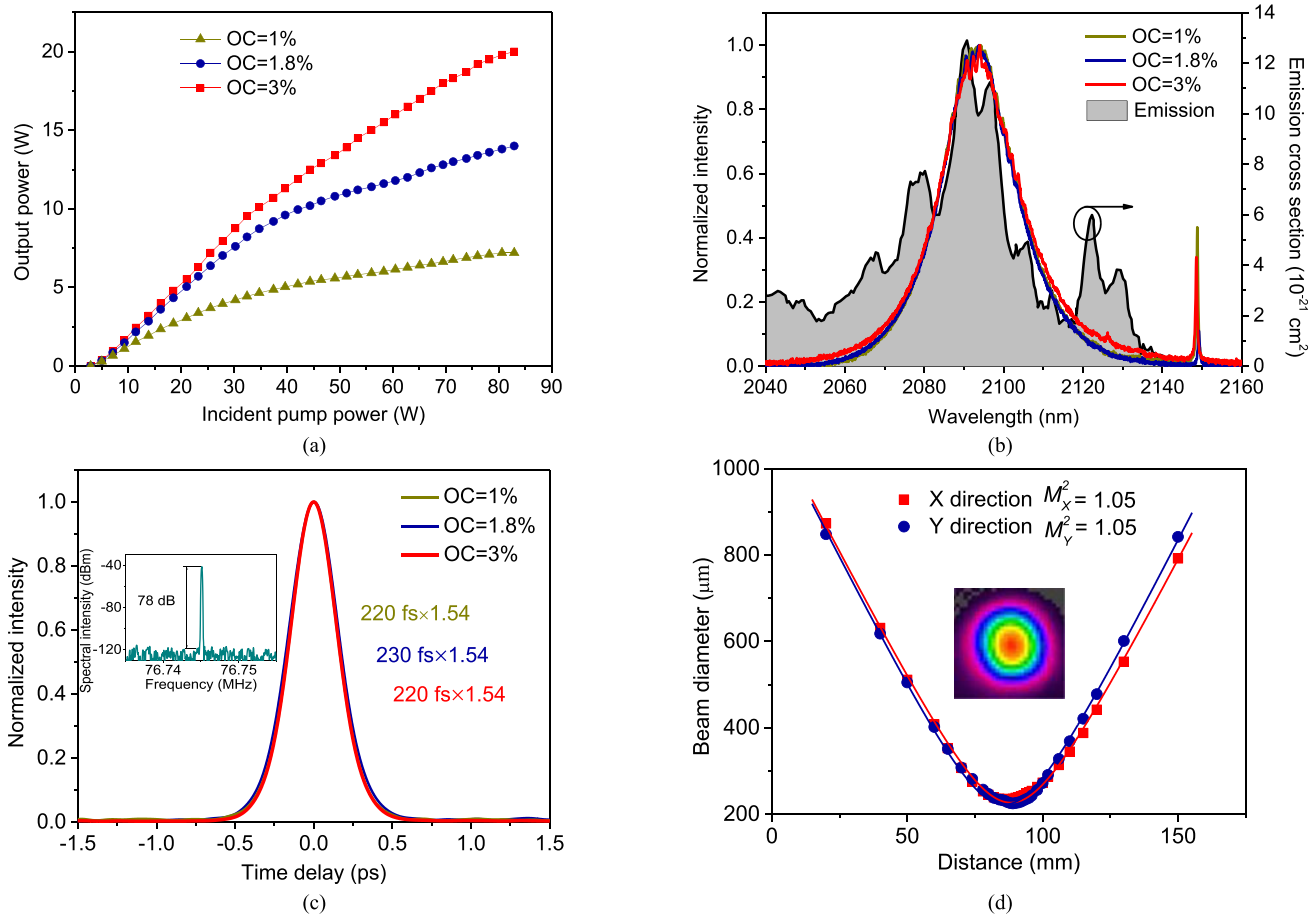

Fig. 7. Output parameters for the eight-pass configuration, pumped by a single Tm-fiber source. (a) CW output power versus incident pump power at three different OCs. (b). Mode-locked spectra. (c) Intensity autocorrelation traces of pulses with different OCs. Inset: Radio frequency spectrum with RBW of 100 Hz in a frequency window of 20 kHz. The spectrum was measured with an OC of 3%. (d) Beam profile and M^2 measurement with an OC of 3%.

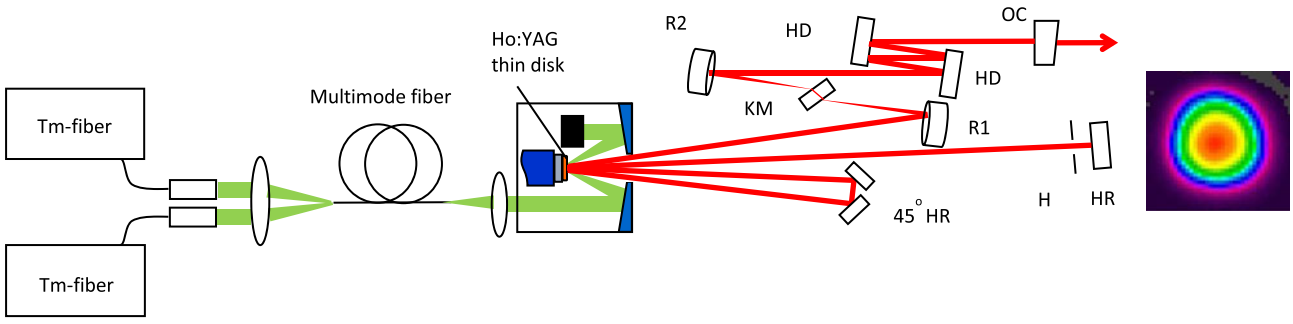

Fig. 8. Schematic of the eight-pass configuration, pumped by two Tm-fiber sources. Right: Beam profile of the oscillator with an OC of 4%.

multimode fiber used for beam homogenization can simultaneously accept, as input, multiple single-mode beams from additional Tm fiber lasers, enabling the scaling of pump power available to the Ho:YAG thin-disk oscillator (see Fig. 8). Using a total of two Tm fiber lasers, the incident pump power can be increased to 110 W, allowing the use of a 4% OC. A CW output power of 29 W was obtained when the oscillator was operated around the stability center, as shown in Fig. 9(a). The oscillator can deliver an average output power of 25 W after it was mode-locked (compared to 23 W in CW before mode locking), corresponding to an optical-to-optical efficiency of 22%. When the power leaked from the two 45-degree mirrors are taken into account, the average power and optical-to-optical efficiency is even higher at 26.6 W and 24% respectively. The mode-locked spectrum and intensity autocorrelation trace are shown in Fig. 9(b) and (c), exhibiting nearly Fourier-transform-limited pulses with a pulse duration of 270 fs. The beat-note signal shown in Fig. 9(d) has a signal-to-noise ratio of 69 dB—lower than previous cases—but still implies a stable mode-locked operation of the oscillator.

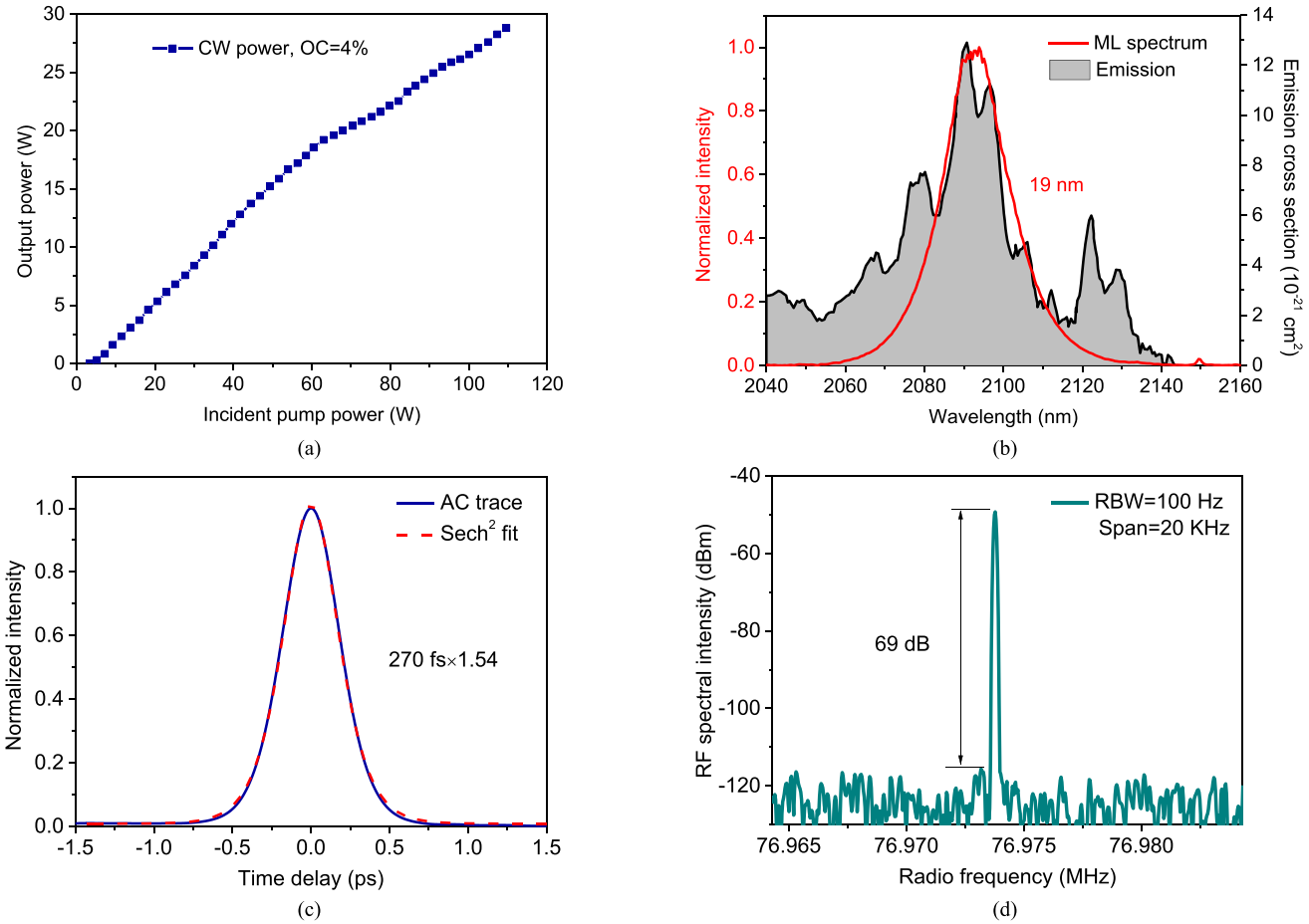

Fig. 9. Output parameters with 4% OC for the eight-pass configuration, pumped by two Tm-fiber sources. (a) CW output power versus incident pump power. (b) Mode-locked spectrum. The Kelly sideband at 2150 nm has a reduced intensity compared to Fig. 7(b), due to the narrower spectral bandwidth of the main pulse. (c) Intensity autocorrelation trace of the pulses. (d) Radio frequency spectrum with a RBW of 100 Hz in a frequency window of 20 kHz.

TABLE I
PARAMETERS OF KLM HO:YAG THIN-DISK OSCILLATORS

Passes	4	4	8	8	8	8
OC	1%	1.8%	1%	1.8%	3%	4%
Pump λ (nm)	1908	1908	1908	1908	1908	1908
P_{avg} (W)	6.2	16 (cw spike)	5.8	12	18.4	25
f_{rep} (MHz)	86	86	77	77	77	77
E_P (nJ)	72	186	75	156	239	325
P_{peak} (MW)	0.15	0.41	0.3	0.6	0.96	1.06
τ (fs)	410	400	220	230	220	270
GDD (fs^2)	−16000	−16000	−16000	−16000	−16000	−16000
$\eta_{O\text{-}O}$	10.6%	19.3%	10.4%	16.7%	22.2%	22%

Pump λ, pump wavelength; P_{avg}, average output power; f_{rep}, repetition rate; E_P, pulse energy; P_{peak}, peak power; τ, pulse duration; GDD, intra-cavity dispersion; η_{O-O}, optical-to-optical efficiency.

A summary of the obtained results under different passes and output couplings are presented in Table I.

IV. DISCUSSION

A. *Influence of Water Vapor Absorption*

The development of high power 2 μm laser systems faces additional challenges compared to near-infrared lasers due to the presence of water vapor absorption bands located around 1.9 μm and 2.7 μm (see Fig. 10). The influence of such absorption is especially acute for oscillators with average intracavity powers reaching kW-levels. In contrast to Tm doped laser systems, which usually lases between 1.9 μm and 2 μm, Ho:YAG laser, which lases further away from the absorption regions, has a considerable advantage for broadband mode locking under ambient condition, in which the results presented in this work

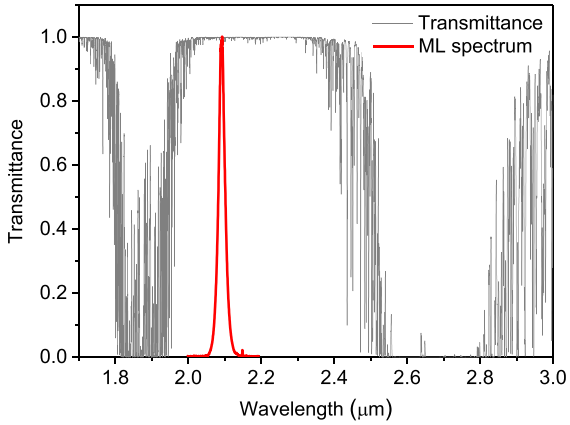

Fig. 10. Water vapor transmittance through 1 meter of gaseous H_2O in the 2 μm range [56].

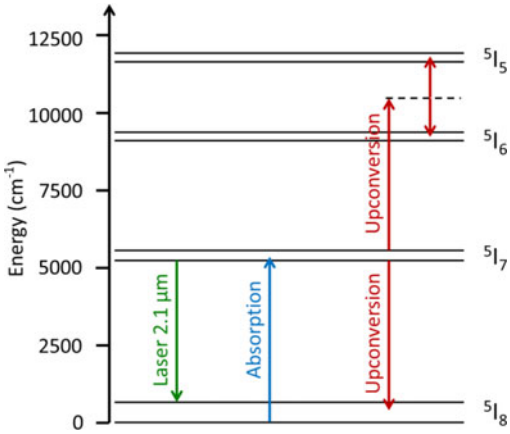

Fig. 11. Energy level diagram of Ho:YAG with the relevant transitions [3].

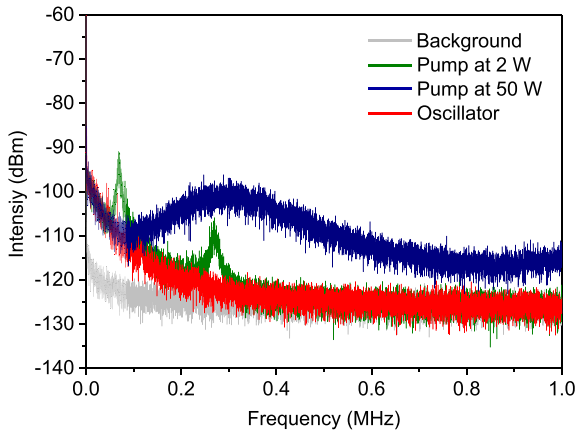

Fig. 12. Qualitative intensity noise measurement below 1 MHz.

were demonstrated. Obviously, operating the laser in a purged or vacuum environment would eliminate the influence of water vapor absorption, and provide several important advantages. Firstly, the reduced absorption and loss for both the pump and lasing wavelengths will increase the operation efficiency. The reduced absorption and the corresponding heat deposition will also help stabilize the temperature inside the laser setup, minimizing any temperature-related drifts from heated mechanical components. Similarly, heat-induced air turbulences in the laser beam path could be eliminated, ensuring the stable running of the laser. Furthermore, the mode-locked spectral width, being able to expand into the previously high loss absorption region, will be broader than in ambient air. Finally, when fully evacuated, any parasitic gaseous nonlinearities in the beam path can be eliminated [55], which is helpful for generating stable high power, high energy pulses. The next-generation Ho:YAG setup will therefore be built under a purged or fully evacuated environment.

B. Upconversion

Instead of using the cross relaxation process of the thulium ions to excite holmium ions, as in the case for traditional Tm-Ho co-doped systems, in this work the Ho:YAG thin-disk was pumped by a Tm-fiber laser at 1.9 μm. This separation of Ho ions from Tm ions eliminates the detrimental process of Ho:Tm up-conversion, in which a Ho atom in the upper manifold of $^5I_7$ is promoted by a nearby Tm atom in the $^3F_4$ manifold to the $^5I_5$ manifold (see Fig. 11). However, for Ho:YAG the interaction between Ho atoms in the $^5I_7$ manifold can also give rise to an up-conversion process. In this Ho:Ho process, two closely spaced holmium ions that are excited into the $^5I_7$ manifold interact with each other, promoting one Ho atom to the $^5I_5$ manifold and demoting the other to the $^5I_8$ manifold. The process is phonon-assisted, non-radiative and becomes pronounced when the population density of the $^5I_7$ manifold is high [57], [58]. Thus it limits the population of holmium ions in the upper laser level and the achievable gain for the crystal. For 2 μm thin-disk lasers, the Ho:Ho up-conversion makes the task of power scaling more difficult due to two conflicting considerations: the necessity to obtain high inversion-levels to compensate for the disk's limited thickness, and the strong up-conversion and excited-state absorption effects at increased inversion-levels. Although the trade-off could be investigated numerically by modeling the rate equations, parameters such as the up-conversion and cross-relaxation coefficients need to be known precisely, and can only be confirmed experimentally. These parameters should be investigated in the future by varying the disk thickness and Ho doping ratios to enable further power scaling.

C. Noise Analysis

For a laser system intended for real applications, the noise characteristic of the output is also a critical parameter. Fig. 12 shows the qualitative intensity noise of the Ho:YAG thin-disk oscillator in the range from 0–1 MHz. It can be seen that the intensity noise of the pump light shifts to higher frequencies and the noise bandwidth broadens when the pump power was increased from 2 to 50 W. Yet the Ho:YAG's oscillator output did not show any obvious intensity noise above 300 kHz even when pumped at 87 W, which can be attributed to the long lifetime of the Ho^{3+} ion (up to 8 ms) filtering out the high frequency

noise. The oscillator shows increased noise towards the low frequency range below 300 kHz, which resulted mainly from two factors:

1) Tm-Fiber Pump Source: The oscillator noise spectrum matches well with that of the pump light below 100 kHz, since the filtering effect of the long lifetime becomes weaker at lower frequencies. Considering that diode lasers have much lower frequency noise than fiber lasers, they are very attractive pump sources for future Ho:YAG thin-disk lasers.

2) The Surroundings: The intensity noise below 100 Hz is attributed to environmental vibrations since the oscillator is built directly onto an optical table with limited isolations from the surroundings. This could be greatly improved by building the oscillator in a monolithic housing in the future [59].

D. Power and Energy Scaling

One of the most advantageous properties of thin-disk technology is its power and energy scalability. Compared to mature Yb:YAG thin-disk oscillators that can deliver several-hundred-watts of ultrafast pulses [34], [35], the development of Ho:YAG thin-disk oscillator has only just begun. The success of high-power and high-energy 1 μm Yb:YAG thin-disk oscillators highlights the opportunity and possible route towards further power scaling for 2 um thin-disk lasers. Specifically for the Ho:YAG thin-disk oscillator, there are several ways to further raise the average power and energy:

1) From experiments, more passes of the laser beam through the gain crystal per round trip can increase the gain and enable the use of higher output coupling ratios. This was implemented by simply extending one of the cavity arms using folding mirrors. However, simply lengthening a cavity arm will change the laser beam mode inside the cavity, and could affect the performance of the laser or its sensitivity to mode-locking, if other parameters such as the size of the pump spot are not adjusted.
2) Another way to increase the number of passes in one round trip is to use imaging concave mirrors, where the extended cavity modes are simply replicas of a section of the original cavity. This allows an increased number of thin-disk passes while keeping the cavity mode unchanged, avoiding the issues mentioned above [60].
3) Since the repetition rate is decided by the cavity length, a longer cavity helps increase the pulse energy under the same average power.
4) The separation of light amplification from the Kerr nonlinearity in our thin-disk oscillator allows us to independently optimize the Kerr lensing effect by choosing suitable materials, thicknesses, the positions of the KM and the mode sizes in the KM. The maximum achievable peak power can be scaled by increasing the mode size in the KM, which could be implemented by changing the curvature of the focusing mirrors in the telescope [34]. By this way the nonlinear phase shift could be maintained even at very high intracavity peak powers.
5) Numerous experiments have been performed at 1 μm wavelength with Yb:YAG thin-disk crystals demonstrating its superior performance for power and energy scaling over other crystalline materials. Not only does Ho:YAG share the same host material and, thus, nearly the same thermo-mechanical properties with Yb:YAG, it also exhibits similarly low quantum defect. However, it remains to be seen whether Ho:YAG disks with higher Ho^{3+} doping and lower thickness (0.1 mm) will significantly increase the output power level.

V. Conclusion

We have demonstrated the first Kerr-lens mode-locked Ho:YAG thin-disk oscillator, where the power was systematically increased by varying the output coupling ratios and the number of passes through the gain medium. The combination of thin-disk geometry, which offers superior thermal control under high power operation, and Kerr-lens mode-locking that effectively provides ultrashort pulse generation led to a number of records in laser development. The pulse duration, at down to 200 fs, is the shortest duration achieved in any Ho:YAG oscillators; the output average power, at up to 30 W, represents a tenfold increase over all previous femtosecond oscillators operating above 1.5 μm wavelength [25], [26]. This combination of ultrashort pulse durations at high average powers has already enabled important applications such as the generation of multi-octave mid-infrared via difference frequency generation in GaSe, a non-oxide nonlinear crystal [9]. Other exciting applications, including the generation of soft X-rays and attosecond pulses for spectroscopy and ultrafast pump-probe experiments will certainly follow in the future. The reported femtosecond Ho:YAG thin-disk oscillator provides a solid foundation for the further development of next-generation 2 μm ultrafast thin-disk lasers, which have the potential to become key enablers in a multitude of research areas.

Acknowledgment

The authors acknowledge the support from Dominik Bauer and Dirk Sutter in TRUMPF Laser GmbH for thin-disk technique and Vladimir Pervak from Ludwig-Maximilians University Munich for providing dispersive mirrors. The authors also acknowledge Prof. Ferenc Krausz in Max-Planck-Institute of Quantum Optics for supporting this work.

References

[1] I. Mingareev *et al.*, "Welding of polymers using a 2 μm thulium fiber laser," *Opt. Laser Technol.*, vol. 44, pp. 2095–2099, 2012.
[2] S. Gravas *et al.*, "Critical review of lasers in benign prostatic hyperplasia (BPH)," *BJU Int.*, vol. 107, pp. 1030–1043, 2011.
[3] K. Scholle, S. Lamrini, P. Koopmann, and P. Fuhrberg, "2 μm laser sources and their possible applications," in *Frontiers in Guided Wave Optics and Optoelectronics*. Rijeka, Croatia: InTech, 2010.
[4] M. Ebrahim-Zadeh and I. T. Sorokina, *Mid-Infrared Coherent Sources and Applications*. New York, NY, USA: Springer, 2008.
[5] F. Silva, S. M. Teichmann, S. L. Cousin, M. Hemmer, and J. Biegert, "Spatiotemporal isolation of attosecond soft X-ray pulses in the water window," *Nature Commun.*, vol. 6, 2015, Art. no. 6611.
[6] J. Weisshaupt *et al.*, "High-brightness table-top hard X-ray source driven by sub-100-femtosecond mid-infrared pulses," *Nature Photon.*, vol. 8, pp. 927–930, 2014.

[7] B. Wolter *et al.*, "Strong-field physics with mid-IR fields," *Phys. Rev. X*, vol. 5, 2015, Art. no. 021034.

[8] H. Pires, M. Baudisch, D. Sanchez, M. Hemmer, and J. Biegert, "Ultrashort pulse generation in the mid-IR," *Prog. Quantum Electron.*, vol. 43, pp. 1–30, 2015.

[9] J. Zhang *et al.*, "Multi-mW, few-cycle mid-infrared continuum spanning from 500 to 2250 cm^{-1}," *Light-Sci. Appl.*, vol. 7, 2018, Art. no. 17180, doi: 10.1038/lsa.2017.180.

[10] M. Seidel *et al.*, "Multi-watt, multi-octave, mid-infrared femtosecond source," *Sci. Adv.*, 2018, accepted for publication.

[11] I. Pupeza *et al.*, "High-power sub-two-cycle mid-infrared pulses at 100 MHz repetition rate," *Nature Photon.*, vol. 9, pp. 721–724, 2015.

[12] V. Petrov, "Parametric down-conversion devices: The coverage of the mid-infrared spectral range by solid-state laser sources," *Opt. Mater.*, vol. 34, pp. 536–554, 2012.

[13] R. A. Kaindl, F. Eickemeyer, M. Woerner, and T. Elsaesser, "Broadband phase-matched difference frequency mixing of femtosecond pulses in GaSe: Experiment and theory," *Appl. Phys. Lett.*, vol. 75, pp. 1060–1062, 1999.

[14] R. Huber, A. Brodschelm, F. Tauser, and A. Leitenstorfer, "Generation and field-resolved detection of femtosecond electromagnetic pulses tunable up to 41 THz," *Appl. Phys. Lett.*, vol. 76, pp. 3191–3193, 2000.

[15] K. L. Vodopyanov, S. B. Mirov, V. G. Voevodin, and P. G. Schunemann, "Two-photon absorption in GaSe and $CdGeAs_2$," *Opt. Commun.*, vol. 155, pp. 47–50, 1998.

[16] F. Junginger *et al.*, "Single-cycle multiterahertz transients with peak fields above 10 MV/cm," *Opt. Lett.*, vol. 35, pp. 2645–2647, 2010.

[17] A. Sell, *Nichtlineare Spektroskopie Mit Einer Hochintensiven Terahertz-Lichtquelle: Wechselwirkungen Mit Ladungsträgern und Spins*. München, Germany: Verlag Dr. Hut GmbH, 2010.

[18] A. A. Lanin and A. M. Zheltikov, "Octave phase matching for optical parametric amplification of single-cycle pulses in the mid-infrared range," *JETP Lett.*, vol. 103, pp. 167–170, 2016.

[19] T. Steinle, F. Mörz, A. Steinmann, and H. Giessen, "Ultra-stable high average power femtosecond laser system tunable from 1.33 to 20 μm," *Opt. Lett.*, vol. 41, pp. 4863–4866, 2016.

[20] M. Engelbrecht, F. Haxsen, A. Ruehl, D. Wandt, and D. Kracht, "Ultrafast thulium-doped fiber-oscillator with pulse energy of 4.3 nJ," *Opt. Lett.*, vol. 33, pp. 690–692, 2008.

[21] P. Li, A. Ruehl, U. Grosse-Wortmann, and I. Hartl, "Sub-100 fs passively mode-locked holmium-doped fiber oscillator operating at 2.06 μm," *Opt. Lett.*, vol. 39, pp. 6859–6862, 2014.

[22] C. Gaida *et al.*, "Thulium-doped fiber chirped-pulse amplification system with 2 GW of peak power," *Opt. Lett.*, vol. 41, pp. 4130–4133, 2016.

[23] F. Stutzki *et al.*, "152 W average power Tm-doped fiber CPA system," *Opt. Lett.*, vol. 39, pp. 4671–4674, Aug. 15, 2014.

[24] S. Vasilyev *et al.*, "Kerr-lens mode-locked middle IR polycrystalline Cr:ZnS laser with a repetition rate 1.2 GHz," in *Proc. Adv. Solid State Lasers Conf.*, 2016, Paper AW1A.2.

[25] S. B. Mirov *et al.*, "Progress in mid-IR lasers based on Cr and Fe-doped II–VI chalcogenides," *IEEE J. Sel. Topics Quantum Electron.*, vol. 21, no. 1, pp. 292–310, Jan./Feb. 2015.

[26] S. Vasilyev *et al.*, "Ultrafast middle-IR lasers and amplifiers based on polycrystalline Cr:ZnS and Cr:ZnSe," *Opt. Mater. Express*, vol. 7, pp. 2636–2650, 2017.

[27] I. T. Sorokina and E. Sorokin, "Femtosecond Cr^{2+} based lasers," *IEEE J. Sel. Topics Quantum Electron.*, vol. 21, no. 1, pp. 273–291, Jan./Feb. 2015.

[28] F. Heine, E. Heumann, G. Huber, and K. L. Schepler, "Mode locking of room-temperature CW thulium and holmium lasers," *Appl. Phys. Lett.*, vol. 60, pp. 1161–1162, 1992.

[29] J. Kwiatkowski, J. Jabczynski, W. Zendzian, L. Gorajek, and M. Kaskow, "High repetition rate, Q-switched Ho:YAG laser resonantly pumped by a 20 W linearly polarized Tm:fiber laser," *Appl. Phys. B*, vol. 114, pp. 395–399, 2014.

[30] K. Mak, S. Groebmeyer, V. Pervak, F. Krausz, and O. Pronin, "Passively mode locked Ho:YAG oscillator at 2.1 μm," in *Proc. Europhoton Conf.*, 2016, Paper PO-3.30.

[31] Y. Wang *et al.*, "Broadly tunable mode-locked Ho:YAG ceramic laser around 2.1 μm," *Opt. Express*, vol. 24, pp. 18003–18012, 2016.

[32] A. Giesen *et al.*, "Scalable concept for diode-pumped high-power solid-state lasers," *Appl. Phys. B*, vol. 58, pp. 365–372, 1994.

[33] J. Brons *et al.*, "Powerful 100-fs-scale Kerr-lens mode-locked thin-disk oscillator," *Opt. Lett.*, vol. 41, pp. 3567–3570, 2016.

[34] J. Brons *et al.*, "Energy scaling of Kerr-lens mode-locked thin-disk oscillators," *Opt. Lett.*, vol. 39, pp. 6442–6445, 2014.

[35] C. J. Saraceno *et al.*, "Ultrafast thin-disk laser with 80 μJ pulse energy and 242 W of average power," *Opt. Lett.*, vol. 39, pp. 9–12, 2014.

[36] D. Bauer, I. Zawischa, D. H. Sutter, A. Killi, and T. Dekorsy, "Mode-locked Yb:YAG thin-disk oscillator with 41 μJ pulse energy at 145 W average infrared power and high power frequency conversion," *Opt. Express*, vol. 20, pp. 9698–9704, 2012.

[37] J. Zhang *et al.*, "High-power, high-efficiency Tm:YAG and Ho:YAG thin-disk lasers," *Laser Photon. Rev.*, vol. 12, 2018, Art. no. 1700273, doi: 10.1002/lpor.201700273.

[38] M. Schellhorn, "Performance of a Ho:YAG thin-disc laser pumped by a diode-pumped 1.9 μm thulium laser," *Appl. Phys. B*, vol. 85, pp. 549–552, 2006.

[39] G. Renz, P. Mahnke, J. Speiser, and A. Giesen, "2 μm Ho:YAG thin disk laser," in *Proc. Adv. Solid-State Photon.*, 2011, Paper AWA24.

[40] J. Speiser, G. Renz, and A. Giesen, "High power thin disk Ho:YAG laser," *Proc. SPIE*, vol. 7912, 2011, Art. no. 79120C.

[41] G. Renz, "Moderate high power 1 to 20 μs and kHz Ho:YAG thin disk laser pulses for laser lithotripsy," *Proc. SPIE*, vol. 9342, 2015, Art. no. 93421W.

[42] G. Stoeppler, D. Parisi, M. Tonelli, and M. Eichhorn, "High-efficient Tm^{3+}:$LiLuF_4$ thin-disk laser," in *Proc. Adv. Solid-State Photon.*, 2012, Paper AW5A.1.

[43] G. Stoeppler, D. Parisi, M. Tonelli, and M. Eichhorn, "High-efficiency 1.9 μm Tm^{3+}:$LiLuF_4$ thin-disk laser," *Opt. Lett.*, vol. 37, pp. 1163–1165, 2012.

[44] A. Diening *et al.*, "High-power Tm:YAG thin-disk laser," in *Proc. Conf. Lasers Electro-Opt.*, 1998, pp. 259–260.

[45] N. Berner *et al.*, "Tm:YAG: A comparison between endpumped laser-rods and the 'thin-disk'-setup," in *Proc. Adv. Solid State Lasers*, 1999, Paper MB3.

[46] S. Vatnik, I. Vedin, and A. Pavljuk, "Diode-pumped thin disk 15% Tm:KYW laser," *Proc. SPIE*, vol. 6731, 2007, Art. no. 673110.

[47] M. Schellhorn *et al.*, "Diode-pumped Tm:Lu_2O_3 thin disk laser," in *Proc. Adv. Solid-State Photon.*, 2011, Paper ATuB14.

[48] S. Vatnik *et al.*, "Thin disk Tm-laser based on highly doped Tm:$KLu(WO_4)_2$/$KLu\ (WO_4)_2$ epitaxy," *Laser Phys. Lett.*, vol. 7, pp. 435–439, 2010.

[49] G. Renz, J. Speiser, and A. Giesen, "2 μm Ho-YAG and Cr:ZnSe thin disk CW lasers," in *Proc. 2nd EOS Top. Meeting Lasers*, 2011.

[50] G. Renz, J. Speiser, A. Giesen, I. Sorokina, and E. Sorokin, "Cr:ZnSe thin disk CW laser," *Proc. SPIE*, vol. 8599, 2013, Art. no. 85991M.

[51] X. Mateos *et al.*, "Holmium thin-disk laser based on Ho:KY$(WO_4)_2$/$KY(WO_4)_2$ epitaxy with 60% slope efficiency and simplified pump geometry," *Opt. Lett.*, vol. 42, pp. 3490–3493, 2017.

[52] A. Diebold *et al.*, "Optimized SESAMs for kilowatt-level ultrafast lasers," *Opt. Express*, vol. 24, pp. 10512–10526, 2016.

[53] T. Amotchkina *et al.*, "Synthesis, fabrication and characterization of a highly-dispersive mirrors for the 2 μm spectral range," *Opt. Express*, vol. 25, pp. 10234–10240, 2017.

[54] J. Zhang *et al.*, "260-megahertz, megawatt-level thin-disk oscillator," *Opt. Lett.*, vol. 40, pp. 1627–1630, 2015.

[55] S. V. Marchese, T. Südmeyer, M. Golling, R. Grange, and U. Keller, "Pulse energy scaling to 5 μJ from a femtosecond thin disk laser," *Opt. Lett.*, vol. 31, pp. 2728–2730, 2006.

[56] [Online]. Available: http://hitran.iao.ru

[57] N. P. Barnes, B. M. Walsh, and E. D. Filer, "Ho:Ho upconversion: Applications to Ho lasers," *J. Opt. Soc. Amer. B*, vol. 20, pp. 1212–1219, 2003.

[58] L. Shaw, R. Chang, and N. Djeu, "Measurement of up-conversion energy-transfer probabilities in Ho:$Y_3Al_5O_{12}$ and Tm:$Y_3Al_5O_{12}$," *Phys. Rev. B, Condensed Matter.*, vol. 50, pp. 6609–6619, 1994.

[59] M. Seidel, J. Brons, G. Arisholm, K. Fritsch, V. Pervak, and O. Pronin, "Efficient high-power ultrashort pulse compression in self-defocusing bulk media," *Sci. Rep.*, vol. 7, 2017, Art. no. 1410.

[60] M. Poetzlberger *et al.*, "Towards active multipass Kerr-lens mode-locked Yb:YAG thin-disk oscillators," in *Proc. Eur. Conf. Lasers Electro-Opt.*, 2017, Paper CA_7_2.

Jinwei Zhang was born in Weihai, China, in 1986. He received the B.S. degree from the Beijing Institute of Technology, Beijing, China, in 2009, and the Ph.D. degree from the Institute of Physics, Chinese Academy of Sciences, Beijing, in 2015.

Under the supervision of Prof. Z. Wei, he developed the interest in solid-state lasers. From October 2013 to May 2015, he was an Exchange Student at the Max Planck Institute of Quantum Optics, Garching, Germany, where he started to explore various techniques on thin-disk lasers. He is currently a Postdoctoral Scientist with Prof. F. Krausz at the Max Planck Institute of Quantum Optics. His current research interests include high-power ultrafast 1- and 2-μm thin-disk lasers and their applications in mid-infrared generation.

Ka Fai Mak was born in Hong Kong in 1986. He received the Masters of Science degree in fiber-based OPOs at high efficiencies from the University of Auckland, Auckland, New Zealand, in 2009, and the Ph.D. degree from the Max Planck Institute for the Science of Light, Erlangen, Germany, and the University of Erlangen-Nuremberg, Erlangen, where he investigated various femtosecond nonlinear frequency conversion techniques involving gas-filled hollow-core photonic crystal fibers with Prof. P. Russell. Since 2015, he has been a Postdoctoral Scientist with Prof. F. Krausz at the Max Planck Institute for Quantum Optics, Garching, Germany. His current research interests include the development of MIR femtosecond sources using various emerging gain media and different nonlinear frequency conversion processes.

Oleg Pronin was born in Ertil, Russia, in 1985. He received the Diploma degree in solid-state physics from the Moscow Engineering Physics Institute (Technical University), Moscow, Russia, in 2008, and the Ph.D. degree in physics from the Ludwig Maximilian University of Munich, Munich, Germany, in 2012.

From 2012 to 2014, he was a Postdoctoral Scientist with the Ludwig Maximilian University of Munich. Since 2014, he has been a Group Leader at the Max Planck Institute of Quantum Optics, Garching, Germany. He has coauthored 24 articles and holds four patents. His research interests include soliton mode locking and instabilities, development of high-power femtosecond 2-μm thin-disk oscillators, ultrabroadband mid-infrared frequency combs, nonlinear effects, Raman self-frequency shifting and supercontinuum generation in soft-glass fibers, carrier-envelope-phase stabilization and few-cycle pulse generation, and optical parametric amplification in mid-infrared.

Dr. Pronin is a recipient of the Springer Thesis Prize.